Physica Scripta. Vol. 2, 216–220, 1970

Analysis of Multi-exponential Decay Curves

L. J. Curtis,[1] H. G. Berry and J. Bromander

Research Institute for Physics, Stockholm, Sweden

Received October 7, 1970

Abstract

Analysis of multi-exponential decay curves. L. J. Curtis, H. G. Berry and J. Bromander (Research Institute for Physics, Stockholm, Sweden).
Physica Scripta (Sweden) 2, 216–220, 1970.

The contributions of cascades to multi-exponential decay curves are analysed. We define the quantitative cascade contribution to an exponential decay as the *replenishment ratio*, which is the ratio of the cascade repopulation rate to the decay depopulation rate. We recommend that this ratio be quoted in future papers on beam-foil or other cascade-affected decay measurements. We also present specific relationships between the fitting parameters and the level populations for decay curves which arise from electric dipole transition schemes of up to second order in cascading. Velocity dispersion effects in beam-foil decays are, in general, shown to be negligible. except for decays from ejected foil-particles.

1. Introduction

At the Second International Conference on Beam-Foil Spectroscopy [1] at Lysekil, in June 1970, much concern was expressed [2] regarding systematic errors in atomic mean lives obtained from cascade-affected time-decay curves. Some techniques for eliminating these errors were suggested, but it was clearly necessary to obtain a precise mathematical estimate of these effects, so that realistic error limits can be obtained for beam-foil data. We have made an analysis of these cascade effects, and conclude that the cascading fraction which produces such systematic errors can be parametrized by a quantity which we define as the *replenishment ratio*. This ratio takes into account both the relative populations of the cascading levels, and their lifetimes, which together affect the reliability of analysis of the resulting decay curve.

We relate the fitted parameters of these cascade-affected decay curves to the initial populations of the levels concerned. These may be obtained only if the branching ratios and cascade schemes are known, but can provide information about the excitation mechanism. For second-order cascade schemes with electric-dipole selection rules, there is a simple separation of the direct and indirect cascading which permits the populations to be evaluated in uncoupled closed formulae.

Finally, we consider velocity dispersion effects in beam-foil decays. The velocity dispersion introduced by the foil interaction with the beam is found to be negligible at most beam energies to an accuracy of better than 3% in the measured decay time. The analysis indicates that even for ejected foil-particles of large velocity dispersion, some decay-time analysis is possible.

2. Cascade contributions to decay curves

The radiated intensity corresponding to a transition from a level i to a level f is given (in photons/sec) by

$$I_{if}(t) = N_i(t) A_{if} \tag{1}$$

where A_{if} is the atomic transition probability and $N_i(t)$ is the instantaneous population of the upper level. For a consecutively labeled cascading level scheme, the populations are governed by a set of coupled differential equations of the form

$$\mathrm{d}N_m/\mathrm{d}t = \sum_{i=m+1}^{r} N_i(t) A_{im} - N_m(t) \alpha_m \tag{2}$$

where α_m denotes the inverse mean life of a level m, obtained by summing A_{mf} over final states f. For notational simplicity in this section, we shall label the transition studied as from an initial level 1 to a final level 0, with $n-1$ cascading levels. It can be shown [3] that Eq. (1) and Eq. (2) imply an intensity variation given by[2]

$$I_{10}(t) = \sum_{j=1}^{n} C_j \exp(-\alpha_j t) \tag{3}$$

where the C_j[3] are defined for some arbitrary time $t=0$. When a mean life $1/\alpha_1$ is determined by curve-fitting techniques, measured values for $I_{10}(t)$ are fitted to $2n$ parameters, corresponding to the C_j and the α_j. Since only α_1 is desired, the other $2n-1$ parameters are often only a hindrance, and are seldom reported unless specific cascade lifetimes are identifiable. It will be shown below how all $2n$ parameters can be utilized to infer (1) the degree of cascading present, and (2) the initial level populations for second-order decay schemes.

2.1. *Quantitative cascade contributions: the replenishment ratio*

The determination of α_1 would be easiest if there were no cascade contributions (i.e., $C_j=0$ for $j\neq 1$). Further, the degree of this contribution is not readily apparent from the raw fitted parameters, as it is a correlated effect of the coefficients and mean lives of all the contributing levels. We develop below an expression which combines the C_j and the α_j in a way which quantitatively reflects their contributions to the measurement of α_1.

To study the population flow for level 1, we can rewrite Eq. (2) in terms of intensities by application of Eq. (1), and apply it to

---

[1] Permanent address: Dept. of Physics and Astronomy, University of Toledo, Toledo, Ohio, USA.

[2] $I_{10}(t)$ is the decay curve of the correlated level scheme, after uncorrelated backgrounds due to unresolved line blending, random noise, etc. have been subtracted. However, the apparent flat background due to very long lived cascades is part of the level scheme, and should not be subtracted.

[3] If $I_{10}(t)$ is instrumentally integrated over some finite time interval Δt, the fitted value of C_j will be averaged in a lifetime dependent manner, and will differ from the true value by a factor $C_j(\text{true})/C_j(\text{fitted}) = (\alpha_j \Delta t/2)/\sinh(\alpha_j \Delta t/2)$. The corrected values $C_j(\text{true})$ should be used in all expressions developed here.

the $1\rightarrow 0$ transition to obtain

$$(\mathrm{d}I_{10}/\mathrm{d}t)/A_{10} = \sum_{i=2}^{n} I_{i1}(t) - \alpha_1 I_{10}(t)/A_{10} \tag{4}$$

The right-hand side of this equation can be interpreted as the difference between the "birth" rate and the "death" rate, where the "births" are due to cascade repopulation (*CR*) and the "deaths" are due to decay depopulation (*DD*). Notice that *DD* is the total depopulation of the level, and not merely the part branching to the particular decay under observation. We therefore define

$$CR = \sum_{i=2}^{n} I_{i1}(t) \tag{5}$$

$$DD = \alpha_1 I_{10}(t)/A_{10} \tag{6}$$

The dynamic behaviour of the level population can be completely described in terms of the birth-to-death ratio, which we henceforth denote as the replenishment ratio, $R = CR/DD$.

If $CR \ll DD$, then $R \ll 1$, the level is essentially unreplenished, and the intensity will vary (at least until R rises) as a single exponential of mean-life $1/\alpha_1$, and cascade effects are negligible. If $CR \cong DD$, $R \cong 1$, and replenishment causes the intensity variation to be strongly multi-exponential, and cascade effects are large. If $CR > DD$, $R > 1$, so that the level is over-replenished, the intensity will show a "growing-in", and cascade effects will dominate (until cascade levels become depleted). The replenishment ratio is therefore a very sensitive and very interpretable measure of the degree of cascade effects. Forming this ratio, we obtain

$$(Rt) = A_{10} \sum_{i=2}^{n} I_{i1}(t)/\alpha_1 I_{10}(t) \tag{7}$$

This can be written entirely in terms of $I_{10}(t)$ using Eq. (4)

$$R(t) = [\alpha_1 I_{10}(t) + \mathrm{d}I_{10}/\mathrm{d}t]/\alpha_1 I_{10}(t) \tag{8}$$

In this form $R(t)$ can be written directly in terms of curve-fitted parameters by substituting Eq. (3) into Eq. (8) to obtain

$$R(t) = \sum_{j=2}^{n} (1 - \alpha_j/\alpha_1)\, C_j \exp(-\alpha_j t) / \sum_{k=1}^{n} C_k \exp(\alpha_k t) \tag{9}$$

Notice that Eq. (9) expresses the replenishment ratio solely in terms of fitted parameters, is independent of the details of the decay scheme[1], and should be the same for all transitions from the same upper level. Cascade contributions can be completely specified by a plot of $R(t)$ versus t over the interval of measurement. Often, long-lived cascades will cause the replenishment ratio to have a smooth monotonic increase, in which case the cascading is well described by the minimum replenishment ratio, evaluated at $t = 0$, and we obtain

$$R(0) = \sum_{j=2}^{n} (1 - \alpha_j/\alpha_1)\, C_j / \sum_{k=1}^{n} C_k \tag{10}$$

For a two-exponential fit this is

$$R(0) = (1 - \alpha_2/\alpha_1)\, C_2/(C_1 + C_2) \tag{11}$$

and for a three exponential fit it is

$$R(0) = [(1 - \alpha_2/\alpha_1)\, C_2 + (1 - \alpha_3/\alpha_1)\, C_3]/(C_1 + C_2 + C_3) \tag{12}$$

Most experimental results to date fit no more than three exponentials. However, at least one measurement [4] has utilized information from the decay curves of the cascade levels in the analysis of a neon transition to reduce the number of free parameters in a 13 exponential fit from 26 to 3. The exponential coefficients and mean lives are presented in Table I. The replenishment ratio for this measurement is 0.54, indicating that, initially, cascades were replenishing about one of every two decays, a fact not easily deduced from the raw fit parameters.

[1] Provided, of course, that the appropriate number of exponential terms are included in the fit.

Table I. *Cascade decomposition of a pulsed electron beam measurement of the $2p_9$–$1s_5$ transition in Ne I (J. L. Kohl, Ph.D. thesis, University of Toledo, Toledo, Ohio, 1969). These coefficients and meanlives infer a replenishment ratio of 0.54*

Term j	C_j	$1/\alpha_j$ (ns)
1	1 400	19.5
2	3 000	195
3	2 500	29.6
4	555	35
5	460	68
6	170	59
7	74	58
8	69	235
9	86	140
10	28	158
11	42	203
12	29	175
13	11	148

The replenishment ratio can also be determined in measurements not employing curve fitting methods. If relative intensities are measured, the ratio can be formed directly with Eq. (7). If excitation is continuous, or modulates about some level, excitation cross-sections and mean lives can be used to determine a secular equilibrium value of the ratio.

2.2. *Level populations from curve fits for second order cascade schemes with electric-dipole selection rules*

Although the presence of cascade level populations can be detrimental to mean life measurements, these populations can provide a valuable study beyond this context. The relative populations present provide information concerning the excitation mechanism, and can be studied as a function of source conditions (beam energy, foil material and thickness etc.). The population distributions with a collisionless sample will generally be quite different from the Boltzmann distribution, and may often be inverted, since radiative de-excitation tends to build up populations in the longer-lived higher-energy states.

It is possible to relate the fitted parameters C_j and α_j to the initial population ratios, if the cascade scheme and the branching ratios A_{jm}/α_j are known [3]. Further, if the mean lives $1/\alpha_j$ are also known, the relative level populations can be determined by fitting the data to the C_j, which is a *linear* fit, and can be made analytically (as opposed to the iterative search routines which must be employed in fitting the α_j). Further constraints can be deduced from the fact that the population ratios must be positive numbers.

In general, the relationships between fitted parameters and populations become quite complicated when higher order cascading is present. However, a striking simplification occurs if we restrict our considerations to second order cascading (i.e., we neglect cascades into level 1 which proceed by three or more steps). Electric-dipole selection rules then divide the cascade levels into two distinct types; direct cascade levels, which have transitions to level 1, and indirect cascade levels, which have transitions to intermediate levels which have direct transitions to level 1.

Selection rules forbid a level from undergoing both direct and indirect transitions to the same level. With this distinction, each direct level d will have a coefficient of the form

$$C_d = \frac{N_d(0)\,A_{d1}\,A_{10}}{(\alpha_1-\alpha_d)} + \sum_{i'} \frac{N_{i'}(0)\,A_{i'd}\,A_{d1}\,A_{10}}{(\alpha_1-\alpha_d)(\alpha_{i'}-\alpha_d)}, \tag{13}$$

where i' is summed over those indirect levels which have transitions to d. Similarly, each indirect level i will have a coefficient

$$C_i = \sum_{d'} \frac{N_i(0)\,A_{id'}\,A_{d'1}\,A_{10}}{(\alpha_1-\alpha_i)(\alpha_{d'}-\alpha_i)}, \tag{14}$$

and here d' is summed over those direct levels which connect level i to level 1. The sum of all coefficients at time $t=0$ must yield the initial intensity, so we have

$$\sum_{j=1}^{n} C_j = N_1(0)\,A_{10} \tag{15}$$

Eqs (13), (14) and (15) can be solved simultaneously to obtain

$$\frac{N_i(0)}{N_1(0)} = \frac{C_i}{\sum_j C_j}\frac{1}{G_i} \tag{16}$$

and

$$\frac{N_d(0)}{N_1(0)} = \frac{C_d}{\sum_j C_j}\left[\frac{(\alpha_1-\alpha_d)}{A_{d1}} + \sum_{i'}\frac{A_{i'd}}{(\alpha_d-\alpha_{i'})\,G_{i'}}\frac{C_{i'}}{C_d}\right] \tag{17}$$

where

$$G_i = [\sum_{d'} A_{id'}\,A_{d'1}/(\alpha_{d'}-\alpha_i)]/(\alpha_1-\alpha_i) \tag{18}$$

where i' is summed over all levels which have transitions into d, and d' is summed over all levels which connect i (or i', where appropriate) indirectly with 1.

As an example of the application of these formulae, consider a sample of hydrogenic atoms, excited so as to be populated in the $n=1$, 2, 3, and 4 levels. The intensity of the Lyman α line ($1s-2p$) will consist of 7 exponential terms, corresponding to the lifetimes of the $2p$, $3s$, $3d$, $4s$, $4p$, $4d$, and $4f$ levels. Transition probabilities for hydrogen are calculable and well known [5], and the contributing values are summarized below. The calculated meanlife of the down transition is $\alpha_{2p}=6.25$, and the meanlives and transition probabilities of the direct transitions are (in $10^8\ s^{-1}$)

$\alpha_{3s}=0.063$ $\quad A_{3s,2p}=0.063$

$\alpha_{3d}=0.64$ $\quad A_{3d,2p}=0.64$

$\alpha_{4s}=0.043$ $\quad A_{4s,2p}=0.025$

$\alpha_{4d}=0.274$ $\quad A_{4d,2p}=0.204$

and for the indirect transitions

$\alpha_{4p}=0.81$ $\quad A_{4p,3s}=0.030$ $\quad A_{4p,3d}=0.003$

$\alpha_{4f}=0.137$ $\quad A_{4f,3d}=0.137$

The computations can easily be done by hand in a few minutes. First we evaluate G_{4p} and G_{4f}. These determine the indirect level population ratios, for which we obtain

$$N_{4p}(0)/N_{2p}(0)=(-394)\,C_{4p}/\Sigma C_j$$

$$N_{4f}(0))/N_{2p}(0)=(35)\,C_{4f}/\Sigma C_j$$

We then apply these to compute the direct level population ratios

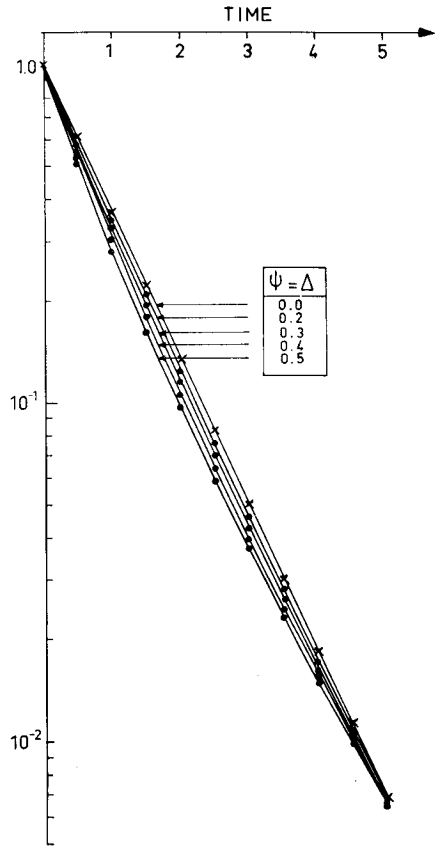

Fig. 1. Intensity decays calculated from Eq. (21). The time-axis is in units of the expected decay time. The decays are normalized to unity at the time zero, and cross again at approximately 5.5 mean lives.

$$N_{3s}(0)/N_{2p}(0)=[(98)\,C_{3s}+(16)\,C_{4p}]/\Sigma C_j$$

$$N_{3d}(0)/N_{2p}(0)=[(9)\,C_{3d}+(7)\,C_{4p}+(10)\,C_{4f}]/\Sigma C_j$$

$$N_{4s}(0)/N_{2p}(0)=(248)\,C_{4s}/\Sigma C_j$$

$$N_{4d}(0)/N_{2p}(0)=(29)\,C_{4d}/\Sigma C_j$$

Population ratios can thus be determined from a 7 parameter linear fit of intensity data to the C_j. In addition, from an examination of these equations we can infer further constraints. Notice that a positive fitted value for C_{4p} would clearly be non-physical, as it would require a negative initial population. Notice also that any significant coefficient for either the $4p$ or the $4s$ level would imply a huge corresponding initial population ratio, so one might ignore these levels, and fit the data to the remaining 5 linear parameters. Since the expressions used here all involve only ratios of transition probabilities, dependences on nuclear charge will cancel, and the expressions are valid for all hydrogenic atoms.

3. Velocity dispersion effects in beam-foil decays

In the analysis of the light intensity decays obtained in beam-foil experiments, it is generally assumed that the emitting particles are all travelling at the same velocity, perpendicular to the observation direction. However, it is known that the foil interaction itself produces a velocity dispersion in the beam. We shall consider two consequences of this velocity dispersion on the intensity decay.

Measurements of the energy distributions of particles after passing through thin carbon foils [6] indicate two important effects. One is an energy loss, and the other is a straggling of the energy distribution. The former is well understood theoretically

Table II. *Effective decay times*

$\psi=\Delta$	t_{min}[a]	t_{max}[b]
0.0	1.00	1.00
0.1	0.99	1.01
0.2	0.95	1,03
0.3	0.90	1.07
0.4	0.85	1.12
0.5	0.79	1.17

[a] t_{min} is derived from the slope between $x=0$ and $x=1$ in Eq. (21).
[b] t_{max} is derived from the slope between $x=4$ and $x=5$ in Eq. (21).

[7] and experimentally [6], and is generally taken account of in accurate beam-foil experiments [1]. The straggling, around the most probable energy loss, is not as well understood [7], and there are few experimental results available [6, 8]. It is the result partly of the statistical nature of the scattering process in the foil, and partly because of the angular dispersion introduced by the scatterings. This angular spreading, which has recently been measured [9–11] and theoretically calculated [12, 13], is also an important factor in determining the velocity distribution observed in the beam-foil decay time measurements.

We shall assume that we are observing a single exponential decay of unit decay time. That is, for particles of velocity v, the light intensity observed at a distance x is $I(x)=I(0)\exp(-x/v)$, where $I(0)$ is the intensity observed at $x=0$.

It has been shown [6] that the electronic scattering in the foil gives rise to an approximately gaussian distribution of velocities, and the closer impact nuclear scattering produces a low energy tail to this distribution. However, for the energy ranges used in beam-foil experiments, the electronic scattering dominates, and it is a good approximation to assume a gaussian velocity distribution about a normalized most probable velocity $v=1$. Then, the number of atoms with a velocity v along the axis is $N(v)\propto \exp[-(v-1)^2/\Delta^2]$, and the observed intensity is

$$I(x)\propto\int_0^\infty e^{-x/v}\,e^{-(v-1)^2/\Delta^2}\,dv \tag{19}$$

where Δ is a measure of the beam-straggling.

The angular spreading of the beam can also be well represented [10] as a gaussian spread into a solid angle $d\Omega$. Thus, at an angle θ, the angular distribution $f(\theta)$ has a velocity $v\cos\theta$ along the beam-axis, and the expected light intensity at a distance x becomes

$$I(x)\propto\int_0^\infty dv\int_0^{\pi/2}2\pi\sin\theta\,d\theta\,e^{-x/v\cos\theta}\,e^{-\theta^2/\psi^2}\,e^{-(v-1)^2/\Delta^2} \tag{20}$$

where ψ is a measure of the angular divergence.

Table III. *Polynomial fits to a decay curve with* $\psi=\Delta=0.5$

x	e^{-x}	$I(x)$[a]	$I'(x)$[b]	$I''(x)$[c]
0.0	1.00	1.00	1.00	1.00
1.0	3.68–1[d]	2.83–1	3.10–1	3.28–1
2.0	13.53–2	9.72–2	10.30–2	10.81–2
3.0	4.98–2	3.68–2	3.70–2	3.62–2
4.0	1.83–2	1.49–2	1.46–2	1.22–2
5.0	6.74–3	6.30–3	6.23–3	4.15–3
6.0	2.48–3	2.78–3	2.78–3	1.42–3

[a] Eq. (21), with $\psi=\Delta=0.5$.
[b] Eq. (22).
[c] Eq. (23), with $\psi=0.5$.
[d] The notation $p-q$ denotes $p\cdot10^{-q}$.

Equation [20] assumes that all particles have the same probability of emitting the photons of interest, independent of their velocity and direction. This may not necessarily be true, particularly when considering very wide velocity distributions such that Δ, $\psi\ll1$ are not good assumptions. Also, we assume that the angular divergence remains within the view of the photon-collecting optics.

If the angular spread is small, then $\sin\theta\cong\theta$, $\cos\theta\cong1-\theta^2/2$, and we can integrate over angles to give

$$I(x)=N\int_0^\infty dv\frac{e^{-x/v}\,e^{-(v-1)^2/\Delta^2}}{1+x\psi^2/2v} \tag{21}$$

where N is a normalization factor.

Equation (21) has to be integrated numerically. Fig. 1 shows some results for different values of ψ and Δ. Measurements [6, 8] of ψ and Δ have shown them to be approximately equal for He, N, and Ne at energies up to 50 keV for C-foils of 5–10 $\mu g\cdot cm^{-2}$. Thus, we have chosen the cases $\psi=\Delta$. For 80 keV $^{16}O^+$ through a 7 $\mu g\cdot cm^{-2}$ C-foil, we find that $\psi=\Delta=0.1$; then, the change in the effective decay time is less than 1%, as seen in Table II. This change is surprisingly small, and it is observed that even for $\psi=\Delta=0.5$, corresponding to a full half-angular-width of 46°, the decay time does not vary by more than 20%.

It is noted that the dispersion-affected curves decay faster for small x, and slower for large x, than the expected decay rate. This is observed in Fig. 1 and Table II, and for equal ψ, Δ the decays all intersect at approximately 5.5 decay times from $x=0$.

Denis et al. [14] have pointed out that the decay of a level which has a cascade of similar lifetime can be approximated by a polynomial coefficient on the decay exponential. Table III shows that the decay with $\psi=\Delta=0.5$ is also well approximated by the polynomial

$$I'(x)=(1-0.19x+0.035x^2)e^{-x} \tag{22}$$

and more approximately, for small x, by

$$I''(x)=(1+\psi^2x/2)^{-1}\cdot e^{-x} \tag{23}$$

Equation (23) is obtained by evaluating Eq. (21) at its principal value.

We conclude that effects of velocity dispersion on decay curves in beam-foil measurements are negligible to the present state of analysis. Thus, at Stockholm, the highest values of ψ, Δ which have been used are $\psi\cong\Delta\cong0.15$ for K at 140 keV, for which Table II shows a less than 3% effect on the measured meanlives [15]. At higher energies the effects become even smaller.

However, velocity dispersion effects are expected to be large for foil-ejected particles [16]. A preliminary application of Eq. (21) to such intensity decays has shown an excellent fit to the data out to 2–3 decay times, with $\psi=0.6$ and $\Delta=0.8$. This corresponds to a half-angular width of 0.5 rad., and a velocity halfwidth of 0.66. At further distances from the foil, an expected high velocity wing gives a tail to the intensity distribution.

4. Acknowledgements

We thank I. Martinson and Wm. Hayden Smith for helpful discussions and are grateful to the Swedish Natural Science Research Council for financial support.

References

1. Beam-Foil Spectroscopy, Proceedings, Nucl. Inst. and Methods, vol. 90 (1970).

2. See Ref. 1., esp. papers by Wiese, W. L., Curtis, L. J., Gaillard, M., Oona, H and Bickel, W. S., and Kay, L.
3. Curtis, L. J., Am. J. Phys. **36**, 1123 (1968).
4. Kohl, J. L., Ph. D. Thesis, University of Toledo (1969).
5. Bethe, H. A. and Salpeter, E. E., Handbuch der Physik XXXV (ed. S. Flügge), p. 352. Berlin, 1957.
6. Fastrup, B., Hvelplund, P. and Sautter, C. A., Mat. Fys. Medd. Dan. Vid. Selsk. **35**, 10 (1966).
7. Lindhard, J., Scharff, M. and Schiott, H. E., Mat. Fys. Medd. Dan. Vid. Selsk. **33**, 14 (1963).
8. Högberg, G., Nordén, H. and Berry, H. G., to be published.
9. Stoner, J. O. and Radziemski, L. J., J. Opt. Soc. Am. **60**, 1108 (1970).
10. Högberg, G., Nordén, H. and Berry, H. G., ref. 1.
11. Kay, L. and Lightfoot, B., ref. 1.
12. Meyer, L., Phys. Stat. Sol., to be published.
13. Bernhard, F., Lippold, J., Meyer, L., Schwabe, S., and Stolle, R. Atomic Collision Phenomena in Solids (ed. D. W. Palmer, M. W. Thompson and P. D. Townsend), p. 663. Amsterdam, 1970.
14. Denis, A., Ceyzériat P., and Dufay, M., J. Opt. Soc. Am. **60**, 1186 (1970).
15. Berry, H. G., Bromander J., and Buchta, R., Physica Scripta **1**, 179 (1970).
16. Berry, H. G., Martinson, I. and Bromander, J., Phys. Letters **31A**, 521 (1970).

Research Institute for Physics
Roslagsvägen 100
S-104 05 Stockholm, Sweden